Structural and transport characterization of AlSb/InAs quantum-well structures grown by molecular-beam epitaxy with two growth interruptions

J. Sigmund,[a] M. Saglam, and H. L. Hartnagel
Institut für Hochfrequenztechnik, Fachbereich Elektrotechnik und Informationstechnik, TU Darmstadt, Merckstr. 25, 64283 Darmstadt, Germany

V. N. Zverev, O. E. Raichev, and P. Debray
Sevice de Physique de l'Etat Condensé, Centre d'Etudes de Saclay, 91191 Gif-sur-Yvette Cedex, France

G. Miehe and H. Fuess
Fachgebiet Strukturforschung, Fachbereich Materialwissenschaft, TU Darmstadt, Petersenstr. 23, 64287 Darmstadt, Germany

(Received 24 October 2001; accepted 18 February 2002)

We have investigated the electron transport properties and the atomic morphology of AlSb/InAs/AlSb quantum wells (QW) grown by molecular-beam epitaxy. Different shutter sequences were used in producing an InSb-like interface. The highest mobility was obtained for a QW width of 15 nm and an InSb-like interface grown by two growth interruptions, one before and one after the deposition of one indium monolayer. For this shutter sequence, several samples with an InAs channel width from 6 to 25 nm were grown and characterized using high-resolution transmission electron microscopy, classical, and quantum Hall measurements. For a channel width less than 15 nm, the interface roughness becomes dominant, leading to a sharp decrease in the electron mobility. The electron effective mass determined by the temperature dependence of the Shubnikov–de Haas oscillazion amplitude is $0.0374m_0$. Transmission electron microscopy images show an atomically abrupt interface and disordered regions directly above the AlSb/InAs interface which can be as large as 2.4 nm. © *2002 American Vacuum Society.* [DOI: 10.1116/1.1468658]

I. INTRODUCTION

InAs quantum wells (QWs) with AlSb or GaSb barriers are nearly lattice matched and are of technological interest for high speed[1,2] and optoelectronic devices.[3]

All structures based on this system have a change of the anions and cations at the interface (IF). Hence, in the case of an AlSb barrier, one has the choice of an AlAs-like or an InSb-like IF, with a great influence on the transport properties.[4] Several authors report that an InSb-like IF results in improved transport properties.[4–7] In practice, one may obtain a mixture of both types, as observed by Ichizli *et al.*[8] The aim of this work was to optimize the growth process to obtain a high-quality InSb-like IF and subsequently study the influence of QW width on the electron mobility.

We have used two different shutter sequences to grow an InSb-like IF and additionally one AlAs-like IF. With the optimized shutter sequence, a set of AlSb/InAs QW structures with QW widths from 6 to 25 nm was grown and characterized by classical and quantum Hall measurements and high-resolution transmission electron microscopy (TEM).

II. EXPERIMENT

The unintentionally doped QW structures were grown on semi-insulating (100) GaAs substrates in a Riber 32 molecular-beam epitaxy with a valved cracker cell for arsenic and a standard cracker cell for antimony to generate molecular beams of As_2 and Sb_2. The oxides are removed at 610 °C prior to the growth of 50 nm GaAs at 580 °C. Then, the substrate temperature is lowered to 460 °C for the GaSb buffer growth. After starting the growth, the surface temperature rises quickly and is kept constant at 485 °C by reducing the substrate thermocouple temperature setpoint. After 500 nm of GaSb growth, the surface temperature becomes constant and the QW growth follows after the temperature is reduced again to 435 °C. Note that the temperature profile depends strongly on the setup (polishing and thickness of the substrate, the substrate holder, and the band pass and emissivity of the pyrometer). While our observations are in agreement with Ref. 9, other groups have observed a temperature peak during GaSb growth on GaAs.[10]

All the QW structures used in this study are grown on substrates polished on one side and mounted on indium-free holders. The surface temperature is measured by an Ircon infrared optical pyrometer with a band pass of 0.91–0.97 μm.

For all grown wafers, the AlSb barrier is 15 nm and the GaSb cap layer is 5 nm thick. First, we investigated the influence of the shutter sequence on the IF. Therefore, two QW structures with an InSb-like IF and two different shutter sequences were grown. An InSb-like bottom IF is commonly grown by closing the Al shutter and exposing the surface for a certain time to an Sb flux (Sb soak).[4,5] Now, we introduced a second growth interruption (GI) right after the growth of the first In monolayer, as shown in Fig. 1.

In this shutter sequence, the first interface is formed by exposing the AlSb layer to 10 s of Sb_2 flux to saturate the surface with Sb. Then one atomic layer of In is deposited. After that, the growth is stopped for another 10 s, and during

[a]Author to whom all correspondence should be addressed; electronic mail: sigmund@hf.tu-darmstadt.de

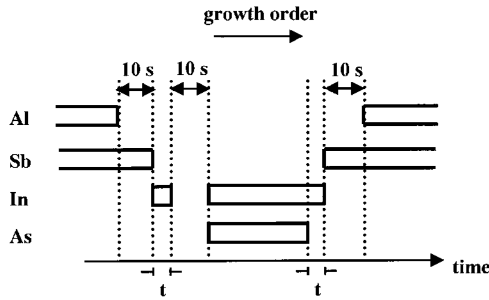

FIG. 1. Shutter sequence for an InSb like interface with two growth interruptions at the first interface.

the last 5 s, the As-valve cracker cell is turned on. This time is needed to open the valve fully. The InAs growth therefore starts directly under As-stabilized conditions. After the growth of the InAs channel, we proceed with the deposition of the second interface with one growth interruption as can be seen in Fig. 1. For comparison purposes, we have grown an additional wafer with an AlAs-like IF and two interruptions at the first IF. These three wafers have an InAs channel width of 15 nm.

In addition, we have investigated the relationship between channel width and transport properties for the two-growth-stop technique. A set of samples with different channel widths ranging from 6 to 25 nm was grown for this purpose.

For the transport property measurements, samples with van der Pauw geometry and In contacts were prepared. Classical Hall measurements were made between 4.2 K and room temperature. Quantum Hall measurements were also carried out to check the two-dimensional character of the electron gas in the quantum wells. Shubnikov–de Haas (SdH) oscillations were measured in a temperature range to determine the electron effective mass. The atomic morphology was studied by high-resolution transmission electron microscopy using a Philips CM200UT, with a resolution of 0.19 nm.

III. RESULTS AND DISCUSSION

Figure 2 shows the electron mobility at 4.2, 77, and 298 K for the various QW structures. For the 15 nm channel width, one can see the influence of the different shutter sequences at the IF. The AlAs-like IF has the lowest mobility, 26100 cm/V s at 4.2 K. Such low mobilities have been reported previously for an AlAs-like IF.[4] An unexpectedly high difference in the mobility was observed between the two wafers with different shutter sequences for an InSb-like interface. Here, the two growth interruptions (2 GIs) lead to a significant improvement in the electron mobility. As the mobility of the unintentionally doped structures increases, the electron sheet density is found to decrease, in the order: 4.85×10^{12} cm^2 (AlAs IF), 3.43×10^{12} cm^{-2} (InSb IF 1GI) to 1.74×10^{12} cm^{-2} (InSb IF 2GI) at 4.2 K. This indicates the reduction of the IF roughness and defect concentration in the same sequence. Additionally, it shows for the 2 GIs that the incorporation of As_{In} antisite defects during the 5 s of the As-valve opening process (the second growth interruption) is negligible. As_{In} antisite defects are expected to act as a source of electrons, similar to As_{Al} antisites.[4] Therefore, their concentration cannot be very high, as the electron density for the InSb IF with 2GI is the lowest one. The higher electron mobility of the structure grown with 2 GIs may be considered to result from the reduction of defect-related scattering centers and interface roughness.

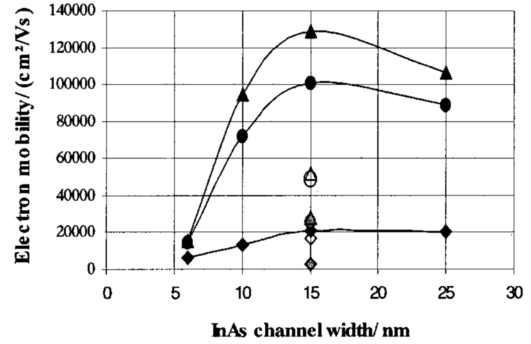

FIG. 2. Electron mobility at three different temperatures in dependence of the InAs channel width and different interface types.

Figure 2 shows the electron mobility dependence on the InAs QW width for structures grown with an InSb-like interfaces with 2 GIs. The mobility decreases rapidly if the QW width is smaller than 10 nm. Quantum Hall measurements carried out on the structure with 15 nm QW width at 70 mK, and shown in Fig. 3, indicate the presence of only one frequency in the SdH oscillations and hence the occupation of only the lowest QW subband. For a channel width less than 15 nm, the interface roughness is therefore the mobility limiting factor. On the other hand, for larger widths, the mobility decreases again which can be due to the population of the second subband and/or the formation of misfit dislocations as a result of the 1.26% lattice mismatch between AlSb and InAs. Indeed, for some structures with QW width 20 nm and higher we observed SdH oscillations with two frequencies and a substantially low electron mobility.

To determine the critical thickness (h_C) for misfit dislocations we used the Matthews and Blakeslee formula:[11]

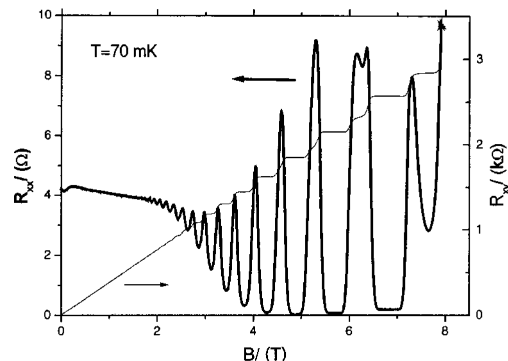

FIG. 3. Results of quantum Hall measurements on a structure with 15 nm QW width grown with 2 GIs.

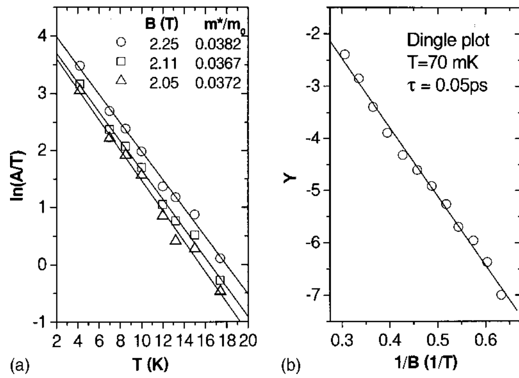

FIG. 4. Temperature dependence of SdH oscillations (a) and the Dingle plot (b). These data were used to determine the electron effective mass and the quantum relaxation time.

$$h_C = \frac{b \cdot \left(1 - \frac{\nu}{4}\right)}{\pi \cdot f \cdot (1+\nu)} \cdot \left(\ln \frac{h_C}{b} + 1\right),$$

with the Poisson ratio $\nu = 0.35$, the Burger's vector $b = 4.28$ Å, and the lattice mismatch $f = 1.26\%$. According to this formula, misfit dislocations should not be present for well widths smaller than 40 nm. For those reasons electron–electron scattering is the most obvious process for the decrease in mobility of the 25 nm InAs sample.

In Fig. 4(a), one can see the temperature dependence of the amplitude of SdH oscillations for different small magnetic fields B for a 15 nm InAs QW sample grown with 2 GIs at the IF. SdH amplitude (A) can be expressed as $A \propto \exp(-\pi\omega_{c\tau 0})\chi/\sinh(\chi)$. Here ω_c is the cyclotron frequency (eB/m^*), τ_0 the quantum relaxation time, and $\chi = 2\pi^2 k_B T/(\hbar\omega_c)$ with k the Boltzmann constant and $\hbar$ the Planck constant.

From Fig. 4(a), the electron effective mass m^* is determined as $(0.0374 \pm 0.002)m_0$. This value is larger than that for bulk InAs ($m^*_{\text{bulk}} = 0.023m_0$), and results to nonparabolicity effects of the conduction band in the QW. According to the three-band Kane model where $m^* = [1 + (2\varepsilon_0 + \varepsilon_F)/\varepsilon_G])m^*_{\text{bulk}}$ (here ε_0 is the size quantization energy, ε_F is the Fermi energy, and ε_G is the energy gap) one obtains for a 15 nm QW an effective mass of $0.033m_0$, which is in reasonable agreement with the measured value.

From Fig. 4(b), the quantum relaxation time is calculated and runs out to be: $\tau_0 \cong 0.05$ ps. Here $Y \equiv \ln[AB \sinh(2\pi^2 k_B T m^*/e\hbar B)]$ and is derived from the definition of the SdH amplitude. As the quantum relaxation time is considerably smaller than the transport relaxation time $\tau_{\text{tr}} = m^*\mu/e \cong 2.7$ ps, one can conclude that τ_0 is determined by small angle scattering.

The atomic microstructure of the IF was investigated by cross sectional high resolution TEM, to investigate any correlation between the transport properties and the microstructure. We observed that roughness at the interface occurs only in the growth direction. Therefore, at the AlSb/InAs IF, the roughness is in the InAs channel, while at the upper IF the roughness is in the barrier. Additionally, the upper IF is found to be smoother than the lower one. These structural properties indicate that for the 2 GIs, the lower IF has a greater influence on the transport behavior than does the upper one, as has been observed by others for 1 GI.[4]

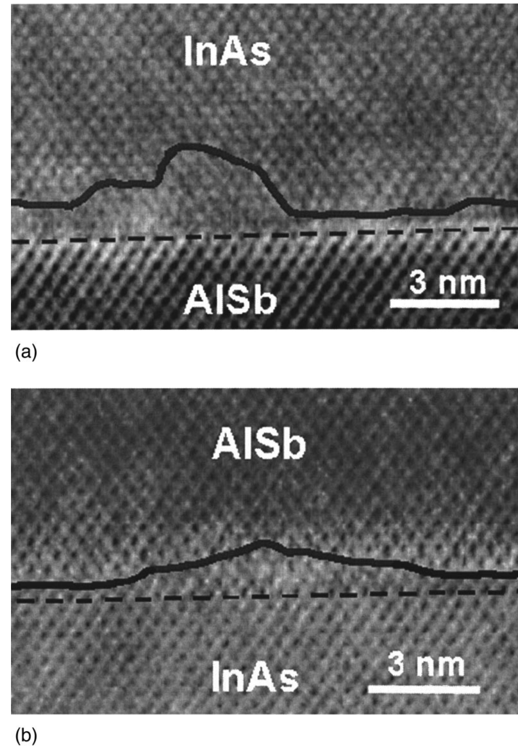

FIG. 5. Cross sectional TEM (XTEM) images showing the (110) plane of (a) the lower AlSb/InAs IF and (b) the upper InAs/AlSb interface. The dashed lines indicate the interfaces and the straight lines the border of the IF roughness.

In Fig. 5, one can see the maximum roughness observed during our TEM investigations for the sample with an 15 nm InAs channel and an InSb-like IF with 2 GIs. The dashed lines indicate the IFs and the straight lines—the border of the IF roughness. Here roughness is defined by regions where the structural perfection is lost, and does not mean that the interface is not atomically abrupt. In Fig. 5(a), one can see an abrupt IF line between AlSb and InAs, but a structural imperfection at the first InAs monolayers.

At both IFs of the 15 nm InAs well [Fig. 5(a): lower IF, Fig. 5(b): upper IF], the roughness occurs in the growth direction as mentioned before. The periodic lattice structure can be seen over the whole upper IF, whereas Fig. 5(a) shows that for the lower IF, some regions exist in which atoms are displaced in sufficient numbers that image contrast is lost. These regions show a tendency towards an amorphous structure and can be as thick as 2.4 nm for the lower IF and 1.3 nm for the upper one. Additionally, the element change is more abrupt for the lower IF.

In conclusion, we have found that one has to distinguish between three types of defects at an interface: three-dimensional defects, or roughness, due to disordered atoms above the IF, one-dimensional defects, which occur as IF steps, due to the change of the elements, and point defects, such as antisites, vacancies, and impurities. These defects at

TABLE I. Hall data at room temperature for AlSb/InAs QWs.

Density/ ($1/cm^2$)	Mobility/ (cm^2/Vs)	*d* InAs/ (nm)	IF	Buffer	Ref. No.
1.40E+12	3 000	5,5	InSb (1Gl)	1 μm GaSb+ 1 μm AlSb+SL	12
1.96E+12	6 400	6	InSb (2Gl)	500 nm GaSb	this work
4.00E+12	4 000	15	AlAs (1Gl)	1 μm GaSb+ 1 μm AlSb+Sl	4
4.55E+12	2 900	15	AlAs (2Gl)	500 nm GaSb	this work
1.05E+12	27 000	15	InSb (1Gl)	1 μm GaSb+ 1 μm AlSb+SL	4
2.51E+12	21 100	15	InSb (2Gl)	500 nm GaSb	this work
4.02E+12	16 500	15	InSb (1Gl)	500 nm GaSb	this work

the IF can act either as electron traps or sources and therefore influence the carrier density. Additionally the electron mobility depends on the defects. If we assume the same atom composition in the observed three-dimensional defects and in the surrounding periodic InAs lattice, an electron moving through a disordered region will be scattered and move on with a lower mobility.

As we changed only the IF growth process, one can conclude that the amount of defects or at least the number of electrically active defects is reduced for the IF grown by 2 GIs, as here the electron density is lower and the mobility higher (Table I).

The defects at an IF will reduce the electron mobility, but on the other hand they may stop dislocations which would otherwise act as scattering centers throughout the well. A dislocation exists only in periodic lattice systems and can be characterized by its Burger's vector, stacking fault, and slip plane. A disordered region or other defects crossing the slip plane may stop the dislocation.

The main dislocation source is due to the strain relaxation process directly above the lattice mismatched substrate. This relaxation process leads to a number of defects which can be seen in Fig. 6 as a bright line (d) parallel to the IF. Additionally, some dislocations starting from there can be seen (a, b, and c).

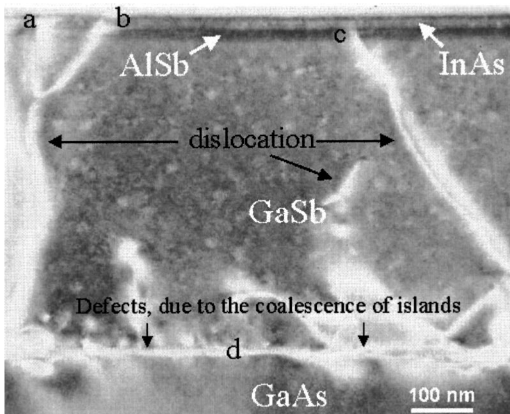

FIG. 6. XTEM image with dislocations starting at the lattice mismatched GaAs/GaSb IF *d*. Dislocations a and b are going through the QW and dislocation *c* is stopped at the AlSb/InAs interface.

As the structures presented here have a buffer layer of only 500 nm thickness, a larger number of dislocations should be present in the well, compared to other reported AlSb/InAs QW structures, where a thicker buffer, for instance 2 μm and a superlattice was used.[4,12] Nevertheless, the Hall data show a high electron density combined with a relatively high mobility, especially for the 2 GI samples, as can be seen in Table I.

Furthermore, one can see in Fig. 6, two dislocations (a and b) going through the InAs channel and a third one (c), which is stopped at the AlSb/InAs IF. During our TEM investigations, we observed 12 dislocations reaching the AlSb barrier, four of them running through the InAs channel, five were stopped at the AlSb/InAs IF, and three at GaSb/AlSb IF. This is a hint that the AlSb/InAs IF with its disordered region stops dislocations more effectively than the GaSb/AlSb IF, where no disordered regions were observed.

A further possible explanation for the higher electron mobility observed for the structures with 2 GIs is that two interruptions at an interface may help to stop dislocations. This is still under investigation.

IV. CONCLUSIONS

A growth process using two growth interruptions at the AlSb/InAs interface has been found to improve the transport properties of AlSb/InAs QW structures. Electron transport measurements show that structures with 15 nm InAs width have the highest electron mobilities. The measured electron effective mass is $(0.0374\pm 0.002)m_0$. High-resolution TEM measurements show disordered regions above the atomically abrupt AlSb/InAs IF. These regions can extend up to 2.4 nm into the InAs.

ACKNOWLEDGMENTS

The authors would like to thank A. Irvin for helpful comments and K. Karova for the sample preparations. This research was partially supported by a grant from the European Commission for the IST project (IST-1999-29012) and the Deutsche Forschungsgemeinschaft (DFG SFB 241 IMES and MEMSTIC).

[1]J. B. Boos, W. Kruppa, B. R. Bennett, D. Park, S. W. Kirchoefer, R. Bass, and H. B. Dietrich, IEEE Trans. Electron Devices **45**, 1869 (1998).
[2]B. Z. Nosho, W. H. Weinberg, W. Barvosa-Carter, A. S. Bracker, R. Magno, B. R. Bennett, J. C. Culbertson, B. V. Shanabrook, and L. J. Whitman, J. Vac. Sci. Technol. B **17**, 1786 (1999).
[3]I. Vurgaftman, J. R. Meyer, F. H. Julien, and L. R. Ram-Mohan, Appl. Phys. Lett. **73**, 711 (1998).
[4]G. Tuttle, H. Kroemer, and J. H. English, J. Appl. Phys. **67**, 3032 (1990).
[5]K. C. Wong, C. Yang, M. Thomas, and H.-R. Blank, J. Appl. Phys. **82**, 4904 (1997).
[6]B. Brar, J. Ibbetson, H. Kroemer, and J. H. English, Appl. Phys. Lett. **64**, 3392 (1994).
[7]B. R. Bennett, B. V. Shanabrook, and E. R. Glaser, Appl. Phys. Lett. **65**, 598 (1994).
[8]V. M. Ichizli, A. Vogt, A. Sigurdardottir, I. M. Tiginyanu, and H. L. Hartnagel, Semicond. Sci. Technol. **14**, 143 (1999).
[9]D. S. Katzer and B. V. Shanabrook, J. Vac. Sci. Technol. B **11**, 1003 (1993).
[10]M. Nouaoura, L. Lassabatere, N. Bentru, J. Bonnet, and A. Ismail, J. Vac. Sci. Technol. B **13**, 83 (1995).
[11]J. W. Matthews and A. E. Blakeslee, J. Cryst. Growth **27**, 118 (1974).
[12]C. R. Bolognesi, H. Kroemer, and J. H. English, J. Vac. Sci. Technol. B **10**, 877 (1992).